

Neuroprotective activity of *Catharanthus roseus* ethanol extract by acetylcholinesterase inhibition and neurite outgrowth studies

ABSTRACT

Aims: To investigate biological activities for neuroprotective effect of *Catharanthus roseus*.

Methodology: *Catharanthus roseus* was identified using DNA barcoding, utilizing *matK*, *trnH-psbA*, and *rbcL* markers. Additionally, thin-layer chromatography (TLC) method was used to analyze the phytochemistry compounds present in the *C. roseus* extracts. Moreover, acetylcholinesterase (AChE) inhibition activity was tested using a modified Ellman's method. Finally, neurite outgrowth activity was determined in rat glial C6 cells treated with varying concentrations of *C. roseus* extracts.

Results: Overall, the plant samples which were collected in Laocai, Vietnam were successfully identified through DNA barcoding regions, using *trnH-psbA*, *matK*, and *rbcL* genes. Phytochemical analysis detected the presence of sterols, terpenoids, flavonoids, polyphenolic in the ethanol extract and its fraction from *C. roseus*. Additionally, the extracts of *C. roseus* displayed remarkably high acetylcholinesterase inhibitory activity. Moreover, the ethanol extract of *C. roseus* shown the most potent neurotrophic activity in a preliminary cell-based screening based on C6 cells neurite outgrowth.

Conclusion: These results demonstrate that *Catharanthus roseus* could be a strong candidate for developing pharmacological drugs to treat neurodegenerative diseases.

Keywords: *Catharanthus roseus*; neurological diseases; AChE inhibitory; neurite outgrowth.

1. INTRODUCTION

Recently, medicinal plants for addressing neurodegenerative diseases and neurological disorders capture the enormous attention from many research groups all over the world [1-3]. *Catharanthus roseus* (L.) G. Don, popularly called the Madagascar periwinkle, was classified as a species of Apocynaceae family [4]. *C. roseus* is cultivated not only for its ornamental beauty in parks, farms, and garden, but is also renowned for its medicinal properties [5]. Having more than 130 discovered compounds, this plant is major source of bioactive substances [6-8]. In traditional folklore systems of medicines, the whole plant consists of leaf, root, flower and seed are usually employed in the treatment of conditions such as hypertension, diabetes, anticancer, and menorrhagia [9]. The extracts of *C. roseus* contain numerous pharmacological features, consist of antimicrobial,

anti-sterility, anthelmintic, antioxidant, antifeedant, and antidiarrheal[10]. Furthermore, vincristine and vinblastine are key compounds acquired from *C. roseus* and exhibit robust anti-neoplastic efficacy in conditions including acute lymphoblastic leukemia, non-Hodgkin's and Hodgkin's lymphomas, breast cancer, Ewing's sarcoma, and other diseases[11]. Additionally, two monomeric Monoterpenoid Indole Alkaloids, ajmalicine and serpentine, derived from its roots, find extensive use in clinical practice for managing circulatory and hypertension disorders[12-15]. In fact, *C. roseus* was revealed neuroprotective activity through acetylcholinesterase inhibition activity by David M. Pereira et al. [16, 17]. However, the molecular mechanisms involved in neuronal protection activity in this effect remain incompletely understood fully.

Alzheimer's disease (AD) stands as the predominant manifestation of dementia, characterized by the accumulation of beta-amyloid (forming amyloid plaques) and the gradual deterioration of microtubules. This leads to the loss of synaptic connections, impaired communication, and the apoptosis of neuronal cells [18]. Although not entirely comprehended, the progression of the disease is believed to be connected to the presence of neurofibrillary tangles and senile plaques. These aggregates are composed of hyperphosphorylated *tau* protein and *amyloid* β ($A\beta$) of varying sizes, respectively [19]. Especially, AD is related to a substantial reduction in the levels of acetylcholine (ACh) due to increased breakdown. ACh is a crucial neurotransmitter responsible for transmitting signals across synapses. After fulfilling its signaling role, ACh is hydrolyzed into choline and acetyl groups through the action of the enzyme acetylcholinesterase (AChE). The utilization of AChE inhibition has been suggested as a promising therapeutic strategy for the management of neurological disorders. The abundance of plants in nature offers a promising source of AChE inhibitors [20, 21].

The implementation of neural-regeneration strategies aiming at reconstructing neuronal and synaptic networks holds potential as a therapeutic approach for AD. Neurogenesis, characterized by neurite outgrowth, is one of the neural-regeneration processes crucial for this purpose. It involves the branching of neurites, subsequent axonal, and dendritic elongation in maturing neurons. This fundamental process plays a vital role in constructing functional neuronal networks and is regarded as a hallmark of neuronal differentiation [22]. Neurite outgrowth serves as a crucial initial step in the formation of the neuronal network. Therefore, drug discovery and development efforts targeted at promoting neurite outgrowth are an essential for understanding molecular mechanisms and developing effective treatments for axonal and synaptic damages [23-25].

The study aimed to investigate the identification *Catharanthus roseus* species, thin layer chromatography (TLC) was utilized to characterize *C. roseus* extracts, elucidating their phytochemical profiles. Moreover, the present study also evaluated the acetylcholinesterase inhibitory activity and neurite outgrowth activity of *C. roseus* extracts. The results of this study more clarified molecular mechanisms of cognitive improvement.

2. MATERIAL AND METHODS

2.1. Collection and identification of *Catharanthus roseus*

We grabbed the samples of *C. roseus* in Sapa, Laocai province in South-west Vietnam in April 2021. The identification of *C. roseus* samples was based on a comparative morphological method following Sunil Kumar et al.'s guidelines[10]. Additionally, DNA barcoding was used, and the nucleotide sequences of the *trnH-psbA*,

matK, and *rbcL* genes were employed for identification purposes. The collected plant samples were dried to a constant weight and stored at temperature of -20 °C for the next experiments.

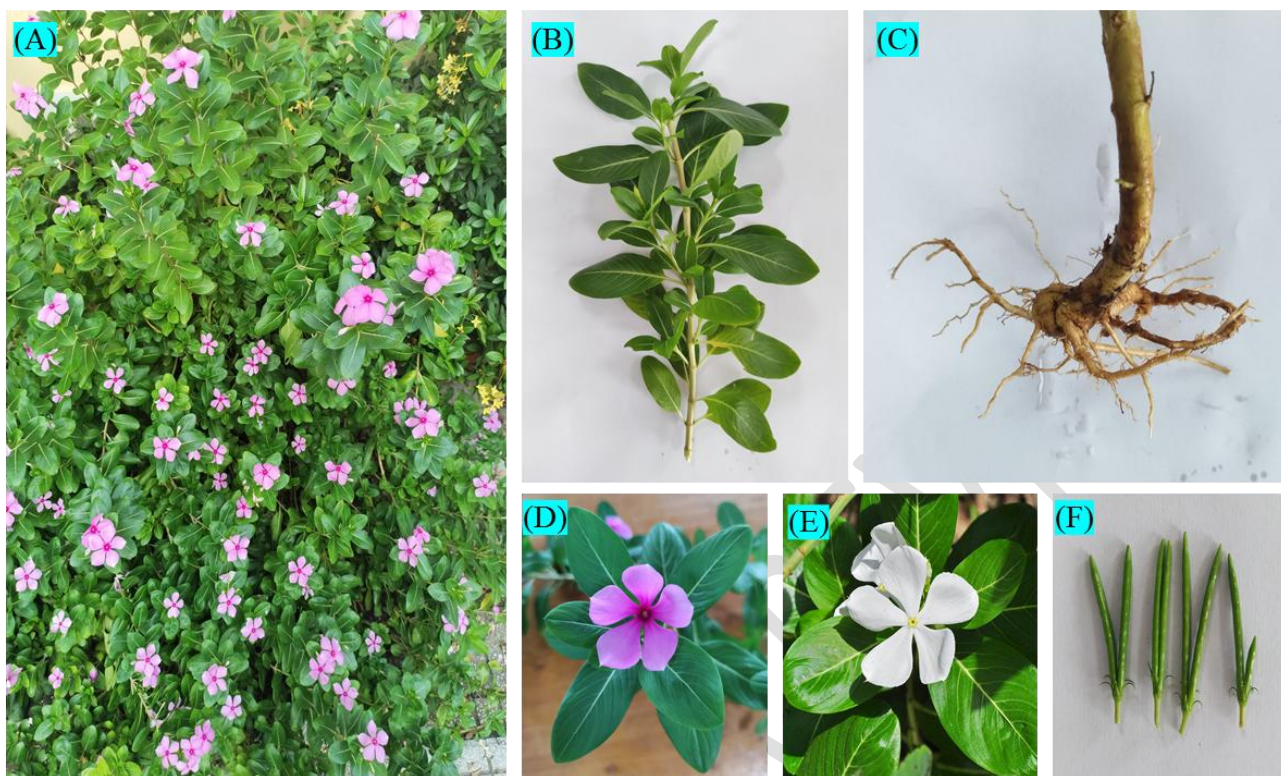


Figure 1. Some morphological characteristic of *Catharanthus roseus*: (A) the whole *C. roseus* plant, (B) stems and leaves of plants at the mature stage, (C) root of *C. roseus*, (D-E) flowers and (F) fruits.

2.2. DNA extraction, PCR amplification, and sequencing for identification of samples

We employed the CTAB method with a slight modification to extract the total DNA of *C. roseus* [26]. Then, we performed the polymerase chain reaction (PCR) amplifications in 20 μ L mixture using Phusa master mix 2x (PhusaBiochem, Vietnam). The primers utilized for sample identification were detailed as follows: *trnH-psbA*(F/R), *matK* (F/R), *rbcL*(F/R) (Table 1). The electrophoresis on a 1% agarose gel was carried out to examine the PCR products and purified using 100% ethanol. The *matK*, *trnH-psbA*, and *rbcL* fragments' nucleotide sequences were determined using Sanger method and analyzed based on the BLAST in NCBI [27].

Table 1. The specific primer for *matK*, *trnH-psbA* and *rbcL* genes in this study

Gene	Primer	Primer sequences(5'-3')	Approximate fragment size (bp)
<i>matK</i>	Forward (F)	ACCGTACTTTTATGTTTACGAGC	883
	Reverse (R)	TCCATCTGGAAATTCGTTCA	
<i>trnH-psbA</i>	Forward (F)	CGCGCATGGTGGATTCAATCC	513
	Reverse (R)	GTTATGCATGAACGTAATGCTC	

<i>rbcL</i>	Forward (F)	GCAAGTGTGGATTCAAAGCTGGTG	573
	Reverse (R)	TGGTTGTGAGTTCACGTTCT	

2.3. Preparation of *Catharanthus roseus* extracts

The whole plant (flower, leave, stem, root, seed) of *C. roseus* were cut off and then freeze-dried for 48 hours. After drying, the samples were soaked in 90% ethanol. The ethanol extract was carried out through refluxing (55 °C-65 °C) and repeated three times. The ethanol solvent was subsequently removed by employing a rotary evaporator to yield the ethanol extract. The liquid-liquid extraction method was used to extract hexane, ethyl acetate, and butanol fractions from the samples following the modified Kwon et al. protocol [28]. Following that, each extract underwent low-pressure vaporization utilizing a rotary evaporator at 55 ± 2 °C).

2.4. Thin layer chromatography (TLC)

We conducted thin layer chromatography (TLC) analysis of all extracts of *C. roseus* using a normal phase TLC plate, according to Supriya Tiwari *et al.* with minimal modification [29]. We utilized normal phase Silica gel 60 F254 HPTLC glass plates measuring 6cm x 6cm (Merck, Darmstadt, Germany) for TLC separations. Chromatographic plates were dried in at 115 °C for 5 min before use. Following, 10 µL of each extract was applied manually as spots to silica gel plates using fine capillary tube. The mobile phase solution for the TLC analysis was optimized by altering its polarity. This was achieved by commencing with the highly non-polar solvent, and subsequently augmenting the polarity. The separated compounds were then visualized under UV light at 254 nm, marked on each TLC plate with a pencil and captured images. Finally, TLC plates were immersed in the Vanillin solution and positioned it on a hot plate preheated to 100 °C until the appearance of visible colored spots.

2.5. Acetylcholinesterase (AChE) inhibitory activity

Each *C. roseus* extract was evaluated AChE inhibition by the modified Ellman's method [30, 31]. Briefly, 10 µL of the sample with different concentrations, 15 µL of 0.1 M phosphate buffer (pH 7.7), 125 µL of 3 mM DTNB and 25 µL of 15 mM ACT1 were mixed. The mixture was placed in an incubator at a temperature of 37°C for 10 minutes. After the pre-incubation, we added 25 µL of enzyme AChE (0.22 U/mL) to the solution and incubated at 37 °C for 15 min. Enzyme activity was measured in a 96-well plate at 410 nm. The inhibition rate was calculated using the following formula:

$$\text{Inhibition rate (\%)} = \frac{A_S - A_B}{A_C - A_B} \times 100, \quad (1)$$

where A_S , A_B , A_C were the absorbance of the investigated extract sample, blank and control samples, respectively. The inhibitory concentrations (IC50) were determined by observing the impact of increasing sample concentrations on inhibition values in the experiment. The positive control used in the experiments was berberine chloride. All the assays were repeated three times [32].

2.6. Maintenance of neuronal cells

The C6 cell line, derived from a rat glial tumor and procured from the American Type Culture Collection (ATCC; MD, USA), the cell culture conditions were described by Samuel Salazar-García *et al.*[33].

2.7.Neurite outgrowth

The human glial C6 cell line was introduced into 24-well plates to reach the population of 8000 cells in each well. The plates, afterwards, was incubated overnight with various non-toxic concentrations of *C. roseus* extracts. Ethanol, ethyl acetate, butanol and hexane extracts of *C. roseus* were added at final concentrations of 5 µg/ml and 2.5 µg/ml. After a 24-hour incubation period, neurite length was observed and measured under 20x magnification using a Nikon Eclipse Ti-U microscope from Japan. At least 5 randomly selected areas (100-200 cells/well) were captured in each well under the microscope (Nikon Eclipse Ti-U, Japan). Within these chosen regions, the length of neurite was examined in a total of 100 cells, employing ImageJ software. The experiments were repeated three times [22].

2.8.Statistical analysis

The results (mean ± standard deviation (SD) were obtained from three separate measurement. We then used both Student's t-test and one-way analysis of variance (ANOVA) to conduct statistical evaluations, within GraphPad Prism 10. The statistical significance of the p-value was considered below 0.05.

3.RESULTS

3.1.The identification of *Catharanthus roseus* species from collected samples in Sapa, Laocai, Vietnam

Plant samples were collected from Sapa, Laocai, Vietnam, in different areas based on morphological characteristics. As shown in Fig. 1 (A-F), the obtained samples were identified as the *Catharanthus roseus* species through a comparative morphological method following by Sunil Kumar *et al.* [10]. Moreover, the samples were molecularly identified using DNA barcoding. The results demonstrated successfully amplification of the medicinal plant samples using primer pairs specific to the three DNA barcoding regions. The nucleotide sequence lengths for the three regions of the *matK*, *trnH-psbA*, and *rbcL* genes in the plant samples are 883 bp, 513 bp, and 573 bp, respectively. The obtained sequences from the collected samples were tested for similarity with the available sequences on Genbank using the BLAST tool. The Fig. 2 (A-B) showed that the sample sequences of the three barcode genes closely aligned with the reference database, indicating high similarity to species in genus *Catharanthus*. Specifically, the *trnH-psbA* region possessed the highest identification efficiency of 99.74% with *Catharanthus roseus* voucher Trotta950331 (GenBank accession number **MH621819.1**), and *Catharanthus roseus* voucher A2424, partial sequence– **MH069885.1**- (99.74%) based on Genbank on the NCBI website. In addition, when comparing the *matK* sequences extracted from the Sapa samples with the *matK* sequence of *Catharanthus roseus* (GenBank accession number **DQ660507.1**), a notable similarity percentage of 99.64% was uncovered. Moreover, similar results were observed with *rbcL* barcode, with a sequence similarity of 99.27% to *Catharanthus roseus (rbcL) gene partial cds* (**MN125628.1**), *Catharanthus roseus* voucher A2424– **MH069755.1** (99.27%), and *Catharanthus sp. yangApY002*– **KX910826.1** (99.27%)

(Fig. 2A-B). These results conclude that the collected medicinal plant samples are members of the genus *Catharanthus*, specifically belonging to the species *Catharanthus roseus*.

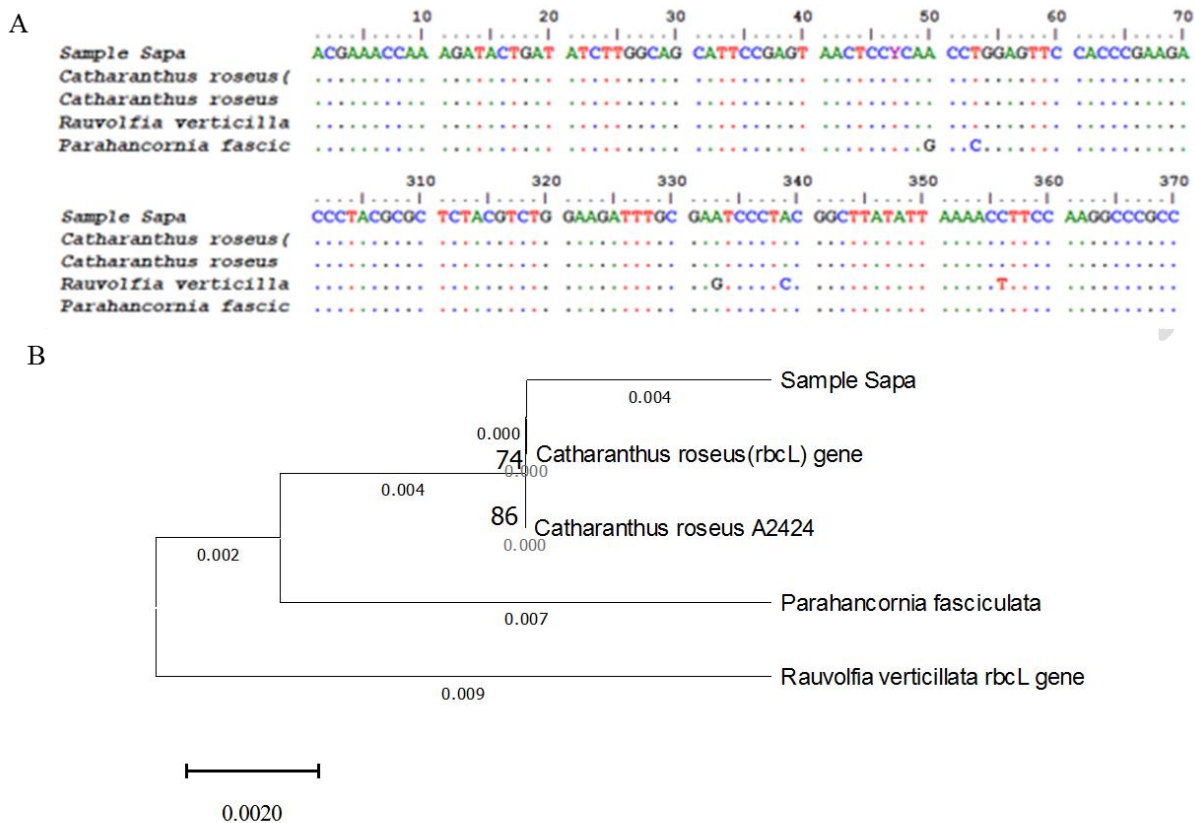


Figure 2. (A) Alignment of ribulose-1,5-bisphosphate carboxylase (rbcL) barcode region of five species. (B) The phylogenetic tree was constructed using the Neighbor-Joining method. The evolutionary distances were computed using the Kimura 2-parameter method and are in the units of the number of base substitutions per site. This analysis involved 5 nucleotide sequences. Evolutionary analyses were conducted in MEGA11.

3.2. Thin-layer chromatography analysis of different fractions of *Catharanthus roseus*

To verify the presence of compounds in *C. roseus* extracts by TLC analysis, five mobile phases were selected for the analyses of extracts: Dichloromethane (DCM): Methanol (MeOH) (7:3, v/v); DCM: MeOH (8:2, v/v) for the more polar butanol extract; DCM: MeOH (9:1, v/v); DCM: Acetone (95:5, v/v); Hexane: Ethanol (9:1, v/v) for the hexane, ethyl acetate and ethanol extract. We utilized Vanillin reagent to assess the content of polyphenols, phytosterols, and terpenoids in the extracts. As shown in Fig. 3A, we examined the developed plates under the UV light with a wavelength of 254 nm before undergoing derivatization. When the plate was exposed to UV light with the 254 nm wavelength, we observed aromatic compounds and highly conjugated systems referring to dark zones against the light-green fluorescence background of the TLC plate. We employed the Vanillin reagent for derivatization to identify a broad range of natural products within the extracts. After the treatment of Vanillin, the plates exhibited violet, blue, red, or green emission, referring to the existence of terpenes, phenols, steroids

andsugars in *C. roseus* extracts(Fig. 3B). Based on the various colors of bands on the TLC plate after derivatization with Vanillin, we can predict the compounds present in the extract samples. In mobile phase (DCM: MeOH (9:1, v/v), a purple band under visible light at 254 nm after derivatization with Vanillin reagent suggest the presence of sterols, terpenoids in extracts at Rf = 0.54, whereas a pink band reveal the existence of flavonoids in *C. roseus* extracts at Rf = 0.75 (Fig. 3B).Hence, the extracts of *Catharanthus roseus* exhibit compounds such as sterols, terpenoids, flavonoids, polyphenolic.

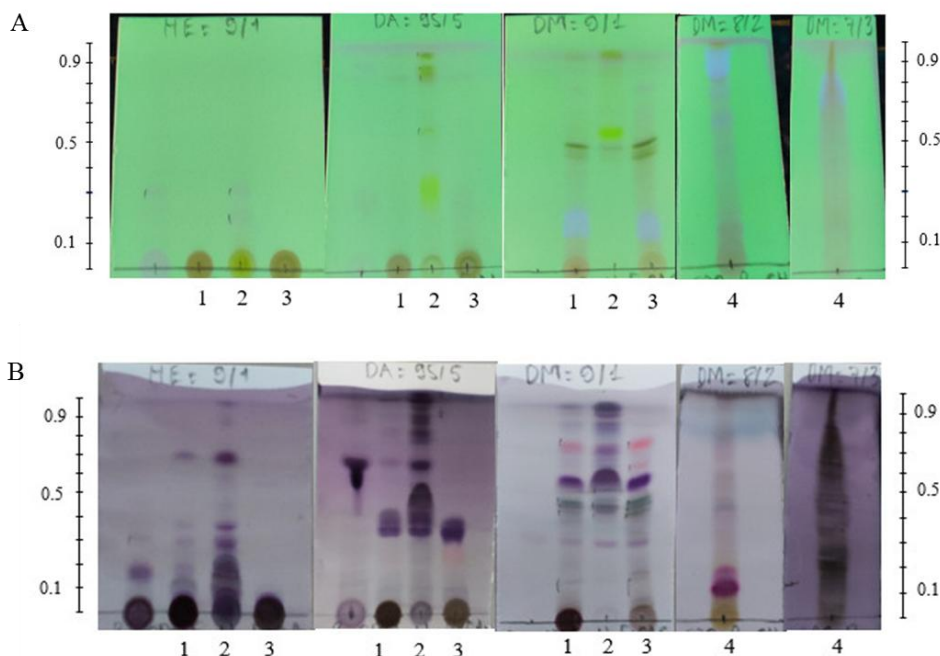


Figure 3. (A) *Catharanthus roseus* extract samples chromatograms viewed under 254 nm. (B) Thin layer chromatography analysis conducted on (1) ethanol, (2) hexane, (3) ethyl acetate, and (4) butanol extract from *Catharanthus roseus* in different solvent systems. H: Hexane; E: Ethyl acetate; D: Dichloromethane; A: Acetone; M: Methanol

3.3. Inhibition of acetylcholinesterase (AChE) by *Catharanthus roseus* extracts

To assess for inhibitors from *C. roseus* extracts, we carried out testing of the AChE inhibitory activities of the extracts using *in vitro* Ellman assay, with berberine chloride as a positive control. The results are presented in Fig. 4. The inhibitory activity of *C. roseus* extracts against AChE showed a dose-dependent pattern. The IC₅₀ determinations confirmed that all four extracts were able to inhibit AChE to different levels, with the following order of potency: Hexane > Butanol > Ethyl acetate > Ethanol > berberine chloride. As shown in Fig. 4, *C. roseus* (ethyl acetate) and *C. roseus* (butanol) extracts inhibited AChE at IC₅₀ values of 212.11 ± 5.24 µg/ml and 331.59 ± 8.47 µg/ml, respectively. *C. roseus* (ethanol) extract exhibited the strongest AChE inhibitory potency, displaying an IC₅₀ value of 10.715 ± 0.82 µg/ml. In contrast, the AChE inhibitory activity of *C. roseus* (hexane) extract was the weakest, demonstrating an IC₅₀ value of 67.546 ± 3.78 µg/ml. These results reveal that *C. roseus* extracts possess activity for AChE inhibition.

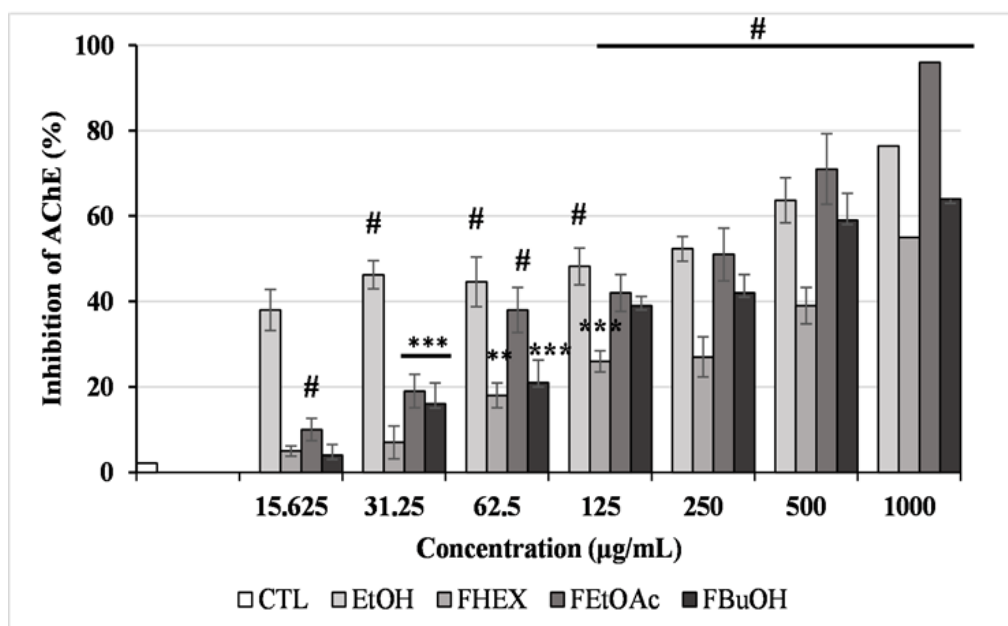


Figure 4. AChE inhibitory activity of *Catharanthus roseus* extracts. The AChE inhibitory activity was evaluated by Ellman's method in presence of ethanol extract (EtOH), hexane fraction (FHEX), ethyl acetate fraction (FEtOAc) and butanol fraction (FBuOH). Data were analysed using the ANOVA test followed by Graphpad prism. Data represented the mean \pm SD. * $p < 0.05$, ** $p < 0.01$; *** $p < 0.001$ and # $p < 0.0001$ is significant differences and percentage inhibition of AChE calculated relative to control (CTL).

3.4. Ethanol extract of *Catharanthus roseus* enhances neurite outgrowth

To evaluate the impact of herbal extracts on neurite outgrowth, the C6 cells were exposed to two distinct concentrations of *C. roseus* extracts (5 µg/ml and 2.5 µg/ml) and observed using a confocal microscope at 20x magnification. As a negative control, dimethyl sulfoxide (DMSO) was employed. Neuronal morphology was observed following treatment with varying concentrations for 24 hours, as depicted in Figure 5A and B. The results showed that *C. roseus* extracts significantly increased the average neurite length compared to 0.1% DMSO control. At a concentration of 2.5 µg/ml, the ethanol extract displayed the highest neurite outgrowth-promoting activities, while the hexane extract showed the lowest neurite outgrowth-promoting activities, with average neurite length of 37.24 ± 3.25 µm and 23.17 ± 1.38 µm, respectively. Similarly, at a concentration of 5 µg/ml, the ethanol extract still had the highest neurite outgrowth-promoting activities, while the butanol extract showed the lowest neurite outgrowth-promoting activities, with average neurite length of 40.62 ± 3.68 µm and 24.83 ± 1.62 µm, respectively (Fig. 5B). The herbal medicinal extracts exhibited a concentration-dependent enhancement in neurite outgrowth-promoting activity. Therefore, the ethanol extract demonstrated the strongest neurite outgrowth-extending activities at both concentrations of 2.5 µg/ml and 5 µg/ml.

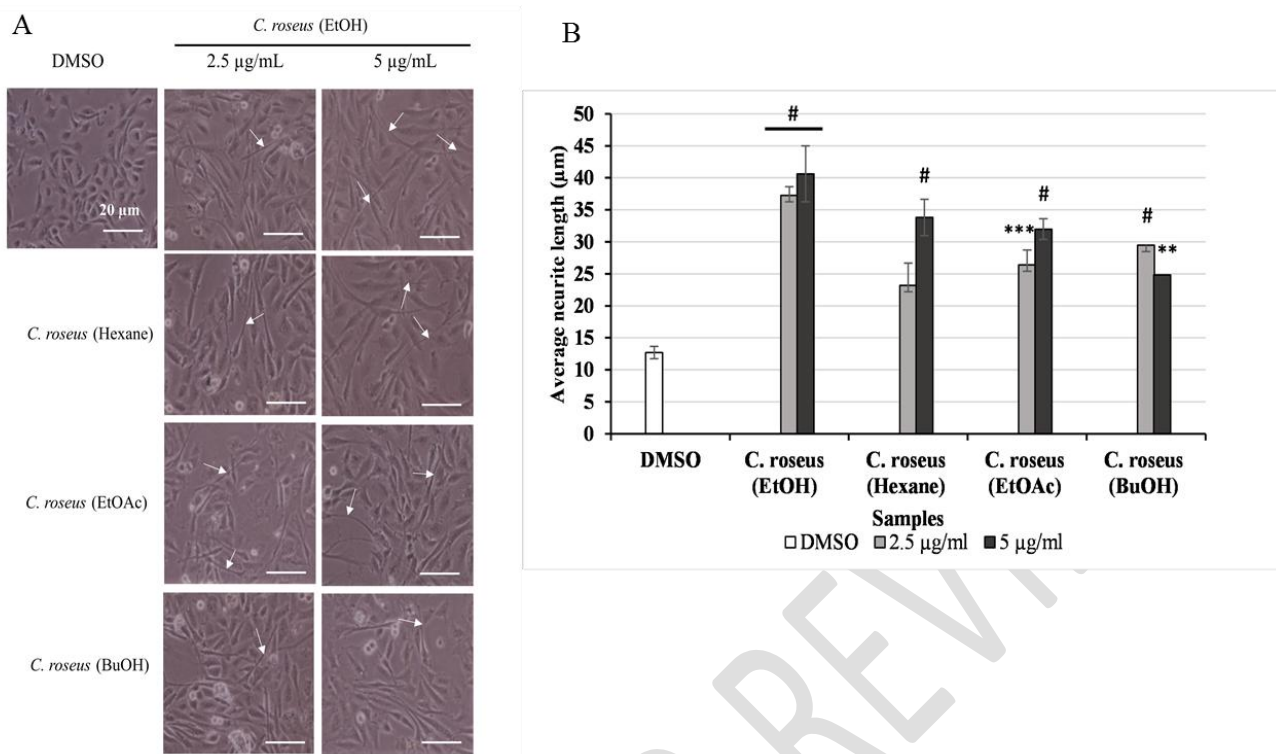


Figure 5. *Catharanthus roseus* extracts for neurite promoting activity in C6 cells. A: Immuno-stained image of C6 cells showed neurite outgrowth following treatment with *C. roseus* extracts (at different concentrations), and 0.1% DMSO (vehicle). Scale bar represents 20 µm. Photomicrographs of representative microscope fields were taken with a 20x objective. B: Graph describing the average length of neurites and optimized concentration of *C. roseus* extracts. Neurites were measured using ImageJ software on bright-field images of C6 cells, taken 24h after treatment. Statistical significance compared with vehicle: * $p < 0.05$, ** $p < 0.01$; *** $p < 0.001$ and # $p < 0.0001$ (ANOVA). Data points represent the mean \pm SD, N=100

4.DISCUSSION

In our study, we present a fast and convenient identification system for plants based on DNA barcoding analysis. We selected three standard barcodes, *trnH-psbA*, *matK* and *rbcL* achieved good species resolution. Through the utilizing of BLAST on NCBI Genbank, the percentage of similarity between the collected sample and the sequences in the NCBI GenBank when employing specific DNA barcoding was *trnH-psbA* > *matK* > *rbcL* at species level. These results indicate that *trnH-psbA* outperforms the other candidate barcodes due to its higher similarity percentage compared to *matK* and *rbcL*. Despite its relatively short sequence length (approximately 513 bp), *trnH-psbA* is recognized as the most polymorphic plastid region in angiosperms. It can be efficiently amplified across a wide spectrum of terrestrial plants, making it capable of distinguishing among a vast quantity of plant species for barcoding applications [34-36]. In previous research, Jian Zhang et al. (2015) indicated the discriminatory capacity of four frequently utilized DNA barcoding markers (*ITS*, *trnH-psbA*, *matK*, and *rbcL*) and their respective multi-locus combinations were investigated using 135 individuals from 33 species of Schisandraceae. The findings revealed that the *trnH-psbA* gene exhibited a greater species-resolving capability

compared to the two coding genes.[37].Furthermore, Maloukhet al. studied DNA barcode on 51 plant species in United Arab Emirates, the *rbcL* marker demonstrated a perfect identification rate, successfully classifying all 51 plant species, which included 11 monocots and 40 eudicots. In contrast, *matK* achieved a correct species identification rate of only 24.45% (14 out of 51)[38]. In a separate study involving Casuarinaceae, it was observed that the *matK* gene provided enhanced resolution compared to *rbcL*[39].In this study, *trnH-psbA* emerged as the most effective molecular barcode for the authentication of *Catharanthus roseus*, with *matK* or *rbcL* serving as supplementary markers. Hence, DNA barcoding has been used to be suitable for this study.

In this report, our TLC method allows to detect the presence of substances in the extracts of *C. roseus* using Vanillin as a derivatization reagent. TLC has consistently demonstrated its superiority as the method of choice, owing to its flexibility, affordability, convenience, and faster analytical capabilities when compared to alternative techniques [40]. TLC profiling of extracts yields compelling indications of the presence of numerous phytochemicals. Different phytochemicals exhibit distinct R_f values in various solvent systems. This diversity in the R_f values of phytochemicals offers valuable insights into their polarity and aids in selecting an optimal solvent system for the purification of pure compounds through column chromatography [41].

Acetylcholine (ACh) serves as a vital neurotransmitter with widespread distribution in the nervous system [42]. AChE is an enzyme that hydrolyzes acetylcholine, occurring in both synapses and neuromuscular junctions, leading to the termination of nerve impulses [43]. Inducing higher levels of ACh in the synaptic cleft through the use of AChE inhibitors stands out as one of the most promising approaches for treating neurological diseases [44]. In this study, *C. roseus* ethanol extract displayed strong AChE inhibition, was measured IC₅₀ at 10.715 ± 0.82 µg/mL (Fig. 4). The activity showed with the ethanol extracts of *C. roseus* was significantly greater than that identified in any plant part in previous studies: stems IC₅₀ = 442; leaves IC₅₀ = 422; petals IC₅₀ = 2683 and roots = 25.5 µg/mL [16, 17]. These results indicate a potency that is 2.5 to 250 folds higher.

5. CONCLUSION

In conclusion, the present study has successfully identified morphological characteristics and DNA barcoding of samples belonging to the *Catharanthus roseus* species. Analysis of the *C. roseus* extracts in various solvents through TLC revealed the presence of major compounds in fractions. Furthermore, these results demonstrated that *C. roseus* extracts have significant potential to improve neuronal survival and exhibited substantial anti-acetylcholinesterase and neurite outgrowth activities. These findings show that *Catharanthus roseus* has the potential to be a promising candidate for developing of pharmacological drugs that can facilitate neuronal regeneration. In the future, our aim is to evaluate the expression of genes and proteins related to its neuroprotective effects in treating neurodegenerative diseases. This will provide valuable insights into the mechanisms responsible for its therapeutic properties, potentially paving the way for novel therapeutic interventions targeting neurological disorders.

REFERENCES

1. More SV, Koppula S, Kim I-S, et al., 2012, The role of bioactive compounds on the promotion of neurite outgrowth, *Molecules*, 17(6), pp. 6728-6753.

2. Duangjan C, Rangsinth P, Zhang S, et al., 2021, Anacardium occidentale L. leaf extracts protect against glutamate/H₂O₂-induced oxidative toxicity and induce neurite outgrowth: The involvement of SIRT1/Nrf2 signaling pathway and teneurin 4 transmembrane protein, *Front Pharmacol*, 12, pp. 627738.
3. Li X-W, Lu Y-Y, Zhang S-Y, et al., 2022, Mechanism of neural regeneration induced by natural product LY01 in the 5×FAD mouse model of Alzheimer's disease, *Front Pharmacol*, 13, pp.
4. Moon SH, Pandurangan M, Kim DH, et al., 2018, A rich source of potential bioactive compounds with anticancer activities by *Catharanthus roseus* cambium meristematic stem cell cultures, *J Ethnopharmacol*, 217, pp. 107-117.
5. Adekomi D, 2015, Madagascar periwinkle (*Catharanthus roseus*) enhances kidney and liver functions in Wistar rats, *European Journal of Anatomy*, 14, pp.
6. Sharma A, Verma P, Mathur A, et al., 2018, Genetic engineering approach using early *Vinca* alkaloid biosynthesis genes led to increased tryptamine and terpenoid indole alkaloids biosynthesis in differentiating cultures of *Catharanthus roseus*, *Protoplasma*, 255(1), pp. 425-435.
7. Sharma A, Verma P, Mathur A, et al., 2018, Overexpression of tryptophan decarboxylase and strictosidine synthase enhanced terpenoid indole alkaloid pathway activity and antineoplastic vinblastine biosynthesis in *Catharanthus roseus*, *Protoplasma*, 255(5), pp. 1281-1294.
8. Mistry V, Sharma A, and Mathur AK, 2021, Confirmation of "pre-plasmolysis mediated ex-osmosis hypothesis" to obtain shoot bud morphogenesis in *Catharanthus roseus*, *Journal of Genetic Engineering Biotechnology*, 19(1), pp. 65.
9. Sharma A, Tiwari P, Arora R, et al., 2022, Madagascar periwinkle alkaloids: biosynthesis, ethnobotanical attributes, and pharmacological functions, *South African Journal of Botany*, 151, pp. 108-115.
10. Kumar S, Singh B, and Singh R, 2022, *Catharanthus roseus* (L.) G. Don: A review of its ethnobotany, phytochemistry, ethnopharmacology and toxicities, *Journal of Ethnopharmacology*, 284, pp. 114647.
11. Sharma A, Mistry V, Kumar V, et al., 2022, Production of effective Phyto-antimicrobials via metabolic engineering strategies, *Current Topics in Medicinal Chemistry*, 22(13), pp. 1068-1092.
12. Sharma A, Tiwari P, Arora R, et al., 2022, Madagascar periwinkle alkaloids: biosynthesis, ethnobotanical attributes, and pharmacological functions, 151, pp. 108-115.
13. Sharma A, Mathur AK, Ganpathy J, et al., 2019, Effect of abiotic elicitation and pathway precursors feeding over terpenoid indole alkaloids production in multiple shoot and callus cultures of *Catharanthus roseus*, *Biologia*, 74, pp. 543-553.
14. Duarte JD and Cooper-DeHoff RM, 2010, Mechanisms for blood pressure lowering and metabolic effects of thiazide and thiazide-like diuretics, *Expert review of cardiovascular therapy*, 8(6), pp. 793-802.
15. El-Sayed M and Verpoorte R, 2007, *Catharanthus* terpenoid indole alkaloids: biosynthesis and regulation, *Phytochemistry Reviews*, 6, pp. 277-305.
16. Pereira DM, Ferreres F, Oliveira JM, et al., 2010, Pharmacological effects of *Catharanthus roseus* root alkaloids in acetylcholinesterase inhibition and cholinergic neurotransmission, *Phytomedicine*, 17(8-9), pp. 646-52.
17. Pereira DM, Ferreres F, Oliveira J, et al., 2009, Targeted metabolite analysis of *Catharanthus roseus* and its biological potential, *Food Chem Toxicol*, 47(6), pp. 1349-54.

18. Alzobaidi N, Quasimi H, Emad NA, et al., 2021, Bioactive Compounds and Traditional Herbal Medicine: Promising Approaches for the Treatment of Dementia, *Degener Neurol Neuromuscul Dis*, 11, pp. 1-14.
19. Balkrishna A, Pokhrel S, Tomer M, et al., 2019, Anti-acetylcholinesterase activities of mono-herbal extracts and exhibited synergistic effects of the phytoconstituents: A biochemical and computational study, *Molecules*, 24(22), pp.
20. Seong SH, Ali MY, Kim HR, et al., 2017, BACE1 inhibitory activity and molecular docking analysis of meroterpenoids from *Sargassum serratifolium*, *Bioorg Med Chem*, 25(15), pp. 3964-3970.
21. Pagliosa LB, Monteiro SC, Silva KB, et al., 2010, Effect of isoquinoline alkaloids from two *Hippeastrum* species on in vitro acetylcholinesterase activity, *Phytomedicine*, 17(8-9), pp. 698-701.
22. Rangsinth P, Duangjan C, Sillapachaiyaporn C, et al., 2021, *Caesalpinia mimosoides* Leaf Extract Promotes Neurite Outgrowth and Inhibits BACE1 Activity in Mutant APP-Overexpressing Neuronal Neuro2a Cells, *Pharmaceuticals (Basel)*, 14(9), pp.
23. Rigby MJ, Gomez TM, and Puglielli L, 2020, Glial Cell-Axonal Growth Cone Interactions in Neurodevelopment and Regeneration, *Frontiers in Neuroscience*, 14, pp.
24. Gao Y, Yan Y, Fang Q, et al., 2019, The Rho kinase inhibitor fasudil attenuates A β 1–42-induced apoptosis via the ASK1/JNK signal pathway in primary cultures of hippocampal neurons, *Metabolic Brain Disease*, 34(6), pp. 1787-1801.
25. Mitre M, Mariga A, and Chao MVJCs, 2017, Neurotrophin signalling: novel insights into mechanisms and pathophysiology, *Clin Sci (Lond)*, 131(1), pp. 13-23.
26. Aboul-Maaty NA-F and Oraby HA-SJBotNRC, 2019, Extraction of high-quality genomic DNA from different plant orders applying a modified CTAB-based method, 43(1), pp. 1-10.
27. NCBI, Basic local alignment search tool (Blast) *Bethesda (MD): National Center for Biotechnology Information*, pp.
28. Seo J-e, Park J-e, Lee J-y, et al., 2016, Determination of seven N-nitrosamines in agricultural food matrices using GC-PCI-MS/MS, *Food analytical methods*, 9, pp. 1595-1605.
29. Tiwari S, Nepal S, Sigdel S, et al., 2020, Phytochemical Screening, Antibacterial- Guided Fractionation, and Thin- Layer Chromatographic Pattern of the Extract Obtained from *Diploknema butyracea*, *Pharmacognosy Research*, 12(4), pp. 437-443.
30. El-Sayed NF, El-Husseyeny M, Ewies EF, et al., 2020, New phosphazine and phosphazide derivatives as multifunctional ligands targeting acetylcholinesterase and β -Amyloid aggregation for treatment of Alzheimer's disease, *Bioorg Chem*, 95, pp. 103499.
31. Youdim MBBJoNT, 2022, Site-activated multi target iron chelators with acetylcholinesterase (AChE) and monoamine oxidase (MAO) inhibitory activities for Alzheimer's disease therapy, 129(5-6), pp. 715-721.
32. Leimann FV, de Souza LB, de Oliveira BPM, et al., 2023, Evaluation of Berberine nanoparticles as a strategy to modulate acetylcholinesterase activity, pp. 113295.
33. Salazar-García S, García-Rodrigo JF, Martínez-Castañón GA, et al., 2020, Silver nanoparticles (AgNPs) and zinc chloride (ZnCl₂) exposure order determines the toxicity in C6 rat glioma cells, *Journal of Nanoparticle Research*, 22(9), pp. 253.

34. Song J, Yao H, Li Y, et al., 2009, Authentication of the family Polygonaceae in Chinese pharmacopoeia by DNA barcoding technique, *J Ethnopharmacol*, 124(3), pp. 434-439.
35. Li H, Xiao W, Tong T, et al., 2021, The specific DNA barcodes based on chloroplast genes for species identification of Orchidaceae plants, *Scientific Reports*, 11(1), pp. 1424.
36. Dev SA, Sijimol K, Prathibha P, et al., 2020, DNA barcoding as a valuable molecular tool for the certification of planting materials in bamboo, *3 Biotech*, 10, pp. 1-12.
37. Zhang J, Chen M, Dong X, et al., 2015, Evaluation of four commonly used DNA barcoding Loci for chinese medicinal plants of the family schisandraceae, *PLoS One*, 10(5), pp. e0125574.
38. Maloukh L, Kumarappan A, Jarrar M, et al., 2017, Discriminatory power of rbcL barcode locus for authentication of some of United Arab Emirates (UAE) native plants, *3 Biotech*, 7(2), pp. 144.
39. Ho VT, Tran TKP, Vu TTT, et al., 2021, Comparison of matK and rbcL DNA barcodes for genetic classification of jewel orchid accessions in Vietnam, *J Genet Eng Biotechnol*, 19(1), pp. 93.
40. Chaudhary SK, Walia V, Singh V, et al., 2020, Thin-layer chromatographic analysis of mangiferin (a bioactive antioxidant from dietary plant sources): a mini-review, *JPC – Journal of Planar Chromatography – Modern TLC*, 33(4), pp. 341-352.
41. Tiwari S, 2022, Phytochemical Screening, Antibacterial-Guided Fractionation and Thin Layer Chromatographic Pattern of the Extract Obtained from *Diploknema butyreaceae*, *Pharmacogn. Res.*, 12, pp. 437-443.
42. Halder N and Lal G, 2021, Cholinergic System and Its Therapeutic Importance in Inflammation and Autoimmunity, *Front Immunol*, 12, pp. 660342.
43. Almehmadi M, Alghamdi S, Asefy Z, et al., 2021, Melatonin hormone as a therapeutic weapon against neurodegenerative diseases, *Cellular and Molecular Biology*, 67(3), pp. 99-106.
44. Marucci G, Buccioni M, Ben DD, et al., 2021, Efficacy of acetylcholinesterase inhibitors in Alzheimer's disease, *Neuropharmacology*, 190, pp. 108352.